

# Constrained information flows in temporal networks reveal intermittent communities

Ulf Aslak\*

*Centre for Social Data Science, University of Copenhagen, DK-1353 København K and  
DTU Compute, Technical University of Denmark, DK-2800 Kgs. Lyngby*

Martin Rosvall†

*Integrated Science Lab, Department of Physics, Umeå University, SE-901 87 Umeå, Sweden*

Sune Lehmann‡

*DTU Compute, Technical University of Denmark, DK-2800 Kgs. Lyngby  
Niels Bohr Institute, University of Copenhagen, DK-2100 København Ø and  
Department of Sociology, University of Copenhagen, DK-1353 København K*

(Dated: November 22, 2017)

Many real-world networks are representations of dynamic systems with interactions that change over time, often in uncoordinated ways and at irregular intervals. For example, university students connect in intermittent groups that repeatedly form and dissolve based on multiple factors, including their lectures, interests, and friends. Such dynamic systems can be represented as multilayer networks where each layer represents a snapshot of the temporal network. In this representation, it is crucial that the links between layers accurately capture real dependencies between those layers. Often, however, these dependencies are unknown. Therefore, current methods connect layers based on simplistic assumptions that cannot capture node-level layer dependencies. For example, connecting every node to itself in other layers with the same weight can wipe out essential dependencies between intermittent groups, making it difficult or even impossible to identify them. In this paper, we present a principled approach to estimating node-level layer dependencies based on the network structure within each layer. We implement our node-level coupling method in the community detection framework Infomap and demonstrate its performance compared to current methods on synthetic and real temporal networks. We show that our approach more effectively constrains information inside multilayer communities so that Infomap can better recover planted groups in multilayer benchmark networks that represent multiple modes with different groups and better identify intermittent communities in real temporal contact networks. These results suggest that node-level layer coupling can improve the modeling of information spreading in temporal networks and better capture their dynamic community structure.

Temporal network representations of dynamic complex systems allow researchers to describe changing interaction patterns. Increasingly, high-resolution interaction data require methods that can simplify and highlight important temporal network structures. An important category of such structures is highly intracommunity groups of nodes, so-called communities. If the nodes represent individuals who alternate between various roles in social temporal networks, the communities will repeatedly form and dissolve at multiple temporal scales and can be described as intermittent. The simplest strategy for identifying intermittent communities is to first separate a temporal network into a sequence of static snapshots, then independently cluster each layer, and finally match the communities across the layers to find the temporal communities [1–6]. Other approaches, including three-way matrix factorization [7], time-node graphs [8], and stochastic block models [7, 9, 10], can directly cluster the multilayer network but are unable to incorporate explicit dependencies between layers. To take into account such interdependencies, some methods cluster multilayer networks using interlayer links that represent specific causal or correlational dependencies between the layers [11–14]. However, explicit interlayer dependencies

are often not available to researchers. Moreover, current approaches for estimating such dependencies by, for example, comparing independently inferred community structure between layers [15], using stochastic block modeling [16], or applying link prediction through cross-validation [17], consider only dependencies between entire layers. In contrast, real systems with multiple and asynchronous recurrent events generate dependencies between layers with varying strength within layers. By ignoring node-level dependencies, current methods ‘wash out’ important dependencies in multilayer networks with intermittent communities at multiple temporal scales.

In this paper, we present a flow-based method that first couples node pairs in different layers based on the similarity between their network neighborhood flow patterns, and then—based on the network structure within layers combined with these node-level interlayer dependencies—identifies temporal communities in the resulting multilayer network. For a single node, non-overlapping neighborhoods are not coupled and identical neighborhoods are maximally coupled. In a social network, the neighborhood flow coupling captures the concept that individuals typically share similar information in similar social contexts. In this sense, neighborhood flow coupling models causal dependencies across time. Finally, we adapt the flow-based community detection algorithm Infomap [18, 19] to make use of this information. We demonstrate the usefulness of neighborhood flow coupling for multilayer community detection on benchmark networks. Additionally, we reveal

\* ulfaslak@gmail.com

† martin@email.edu

‡ sljo@dtu.dk

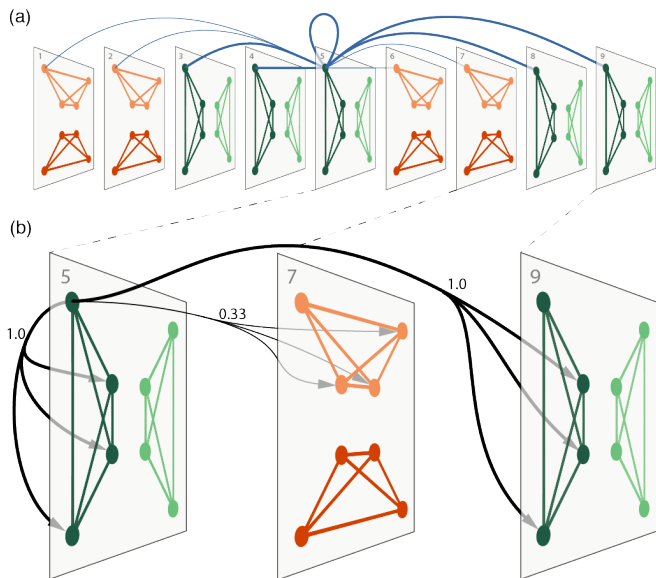


FIG. 1. **Neighborhood flow coupling between a state node and its sibling states in a multilayer network.** (a) Interlayer coupling from the top left state node in layer 5 to all state nodes of the same physical node. State nodes with more similar intralayer outlinks couple more strongly, indicated by the stroke width. (b) Interlayer links are directed and connect a state node to neighbors of state nodes of the same physical node, with weight proportional to the coupling strength and the intralayer link weight of the neighbor node (Eq. 1).

and visualize the temporal evolution of intermittent communities in two temporal human contact networks [20, 21]. While our method targets intermittent communities in temporal contact networks represented by multilayer networks, it nevertheless outperforms other methods in standard benchmark tests on multilayer networks.

## METHODS

In complex networks, groups of nodes in which flows stay for a long time provide a useful notion of communities [18, 22]. Such communities also can provide straightforward generalizations to multilayer networks [13]. We use multilayer networks with *physical* nodes and *state* nodes. Physical nodes represent system components, while state nodes, one for each physical node and layer, represent constraints on flows (see Fig. 1). Accordingly, we consider multilayer communities to be groups of state nodes that capture flows for a significantly long time. In this way, assigning a physical node’s state nodes to different communities naturally results in overlapping communities.

In real-world temporal networks, communities often form and dissolve multiple times with a shorter presence than absence [6]. From the perspective of the entire network, these intermittent communities are often asynchronous in the sense that each community forms and dissolves independently in time relative to other communities. Examples of intermittent communities include group voting trends in the US

Senate [11], time-dependent sets of correlated financial assets [14], social cores in contact networks [6], and modules of coherently active brain areas [23]. Because nodes in these intermittent communities are not able to share information across their long absent times—since nodes are unlikely to be connected—current methods for identifying communities with long flow-persistence times cannot effectively capture the potential for information transfer. A causal dependency across time requires that interlayer link strengths represent the degree to which information is likely to flow between state nodes in adjacent as well as distant layers. Some existing methods indeed evaluate dependencies between layers, but they do it by coupling entire layers [15–17]. There are two important drawbacks to this approach. First, coupling a physical node’s state nodes across all layers generates a large number of links, resulting in computational challenges. For example, in a network with  $n$  nodes in  $t$  layers with average degree  $\langle k \rangle$ , we need  $\langle k \rangle t^2 n$  links in addition to the within-layer links in order to represent connections between state nodes. Second, for large networks with many time slices and intermittent and asynchronous communities, the uniform interlayer links can also dilute community boundaries and aggregate distinct communities (we will discuss this point in detail below). To counter these drawbacks of uniform linking, we propose interlayer dependencies at the node level. By forming state-node-specific interlayer links, neighborhood flow coupling generates high-resolution yet sparse multilayer networks that can capture intermittent communities.

## Neighborhood flow coupling

The goal of our flow-based approach is to enable interlayer coupling based on the local structural properties of the multilayer network. Each layer’s intralayer link structure represents the constraints on network flows at a given time or state of the system. Specifically, we model the network flows in each layer with a random walker that moves from state node to state node guided by the outgoing intralayer links. Because the links represents where flows can move, similar outgoing intralayer link flows in two state nodes of a physical node suggests that the state nodes represent similar states of the physical node. In a social setting, for example, the same group of people may meet again and take up where they left off last time they met. More precisely, the more similar the within-layer flow patterns are, the less would the constraints change and the less would information be lost if the two state nodes were lumped together. We use this information loss measure to couple layers: The less information that is lost if the state nodes were combined, the stronger the interlayer coupling between the state nodes.

This neighborhood flow coupling based on the information loss from merging state nodes is accurately captured by the Jensen-Shannon divergence. In detail, for neighborhood flow coupling between physical node  $i$ ’s state nodes in layers  $\alpha$  and  $\beta$ , the state nodes’ normalized intralayer outlinks  $P_i^\alpha$  and  $P_i^\beta$

give their coupling strength  $D_i^{\alpha\beta}$ ,

$$D_i^{\alpha\beta} = 1 - \text{JSD}(\mathbf{P}_i^\alpha, \mathbf{P}_i^\beta) \quad (1)$$

$$= 1 - H\left(\frac{1}{2}\mathbf{P}_i^\alpha + \frac{1}{2}\mathbf{P}_i^\beta\right) + \frac{1}{2}H(\mathbf{P}_i^\alpha) + \frac{1}{2}H(\mathbf{P}_i^\beta), \quad (2)$$

where  $\text{JSD}(\cdot, \cdot)$  is the Jensen-Shannon divergence and  $H(\cdot)$  is the Shannon entropy. In a multilayer network with neighborhood flow coupling, a random walker moves from state node to state node within a layer guided by the intralayer links and, at rate  $r$ , jumps to another layer proportional to the intralayer link similarity between the state nodes (see Fig. 1a).

While the interlayer coupling connects state nodes of the same physical node, the interlayer links connect to their neighbors. That is, a random walker at a state node of physical node  $i$  in layer  $\alpha$ ,  $(i, \alpha)$  for short, remains in the same layer with probability  $1 - r$  and moves to state node  $(j, \alpha)$  with probability proportional to the intralayer link weight  $W_{ij}^\alpha$ , or relaxes the layer constraint with probability  $r$ , switches to layer  $\beta$  proportional to the interlayer coupling strength  $D_i^{\alpha\beta}$ , and moves to state node  $(j, \beta)$  proportional to the intralayer link weight  $W_{ij}^\beta$ . Consequently, with intralayer out-strength  $s_i^\beta = \sum_j W_{ij}^\beta$  and interlayer out-strength  $S_i^\alpha = \sum_\beta D_i^{\alpha\beta}$  of state node  $(i, \alpha)$ , the transition probabilities as a function of  $r$  are

$$P_{ij}^{\alpha\beta}(r) = (1 - r) \frac{W_{ij}^\beta}{s_i^\beta} \delta_{\alpha\beta} + r \frac{D_i^{\alpha\beta}}{S_i^\alpha} \frac{W_{ij}^\beta}{s_i^\beta}, \quad (3)$$

where  $\delta_{\alpha\beta}$  is the Kronecker delta. Therefore, relaxing the layer constraint means that the random walker loses memory of which layer it is currently visiting and instead follows the outgoing links of another state node of the same physical node. With uniform interlayer coupling, relaxing the layer constraint corresponds to a step on the fully aggregated network. However, neighborhood flow coupling takes advantage of higher-order information in the multilayer network that enables longer persistence times in intermittent communities (see Fig. 1b).

### Neighborhood flow coupling and the map equation

To use neighborhood flow coupling in the context of community detection, we use the map equation framework for multilayer networks [13, 19]. For our purposes, the map equation framework comes with two advantages. Firstly, the map equation is flow-based and directly integrates state-node-specific interlayer flows, as it balances intralayer and interlayer flows by relaxing the intralayer constraints with an interlayer relax rate. Secondly, the map equation naturally clusters coupled state nodes with similar intralayer links in the same community, as it assigns state nodes of the same physical node and community to the same codeword to capture the fact that they represent the same physical object. Therefore, the flow-based and information-theoretic nature of the map equation is a good fit with neighborhood flow coupling.

In detail, for a two-level modular description of flows from node to node in  $m$  communities, one *index codebook* contains the community-enter codewords and  $m$  *module codebooks* contain the node-visit and community-exit codewords within modules. Each codebook's average codeword length is given by the Shannon entropy of their rates of use,  $Q$  for enter codewords with total rate of use  $q_\curvearrowright$ , and  $\mathcal{P}_j$  for codewords in community  $j$  with total rate of use  $p_{j\curvearrowleft}$ . For node partition  $M$ , the map equation therefore takes the form

$$L(M) = q_\curvearrowright H(Q) + \sum_{j=1}^m p_{j\curvearrowleft} H(\mathcal{P}_j). \quad (4)$$

Applied to a possibly weighted and directed network, Infomap searches for the node partition  $M$  that minimizes the map equation and reveals the most modular regularities in the network flows.

The map equation remains the same for multilayer networks, with one important generalization: when state nodes of the same physical node are assigned to the same community, they are assigned a common code word derived from their total visit rate. This coding scheme captures the very essence of multilayer networks, that all state nodes of the same physical node represent the same physical object [13].

We have implemented the neighborhood flow coupling in the Infomap software package available on [www.mapequation.org](http://www.mapequation.org).

## RESULTS

We first validate the performance of Infomap with neighborhood flow coupling on benchmark networks with a multilayer structure. Then we identify temporal communities in two face-to-face contact networks.

### Performance tests on benchmark networks

We compare neighborhood flow coupling with other (existing) interlayer coupling schemes on three types of multilayer benchmark networks. This strategy allows us to test each method's ability to handle overlapping community structure, recover communities in increasingly sparse multilayer networks, and retain flows within intermittent communities. We compare neighborhood flow coupling (NFC) with full coupling (FC), adjacent coupling (AC), and no-coupling (NC). Full coupling with uniform coupling across layers and no coupling with only the intrinsic coupling from the multilayer coding scheme are extreme cases of neighborhood flow coupling, when the structural similarity in Eq. (1) is either 1 or 0 across all state nodes of the same physical node [13]. Adjacent coupling with uniform coupling strength to the nearest layers is an appealing method for gradually changing communities, but cannot capture intermittent communities. These alternative coupling methods provide references which we can use to compare and contrast the results of neighborhood flow coupling.

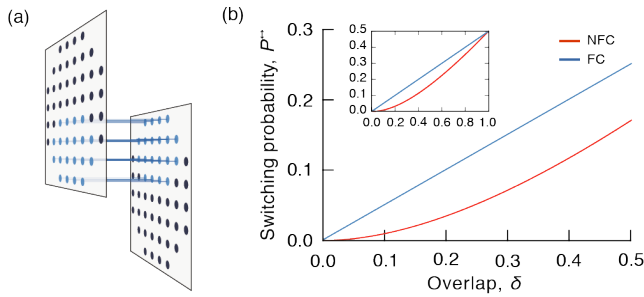


FIG. 2. **Coupling strength as a function of overlap.** (a) A simple conceptual model with two identical fully connected communities of size  $N$  that overlap by  $\delta N$  nodes. Overlapping nodes are in blue. (b) Layer switching probability for full and neighborhood flow coupling as functions of overlap. The inset shows the full range from 0 to 1. For large overlaps, the layer switch rates of the two methods converge.

### Community overlap

In real networks, such as face-to-face networks, communities are rarely completely non-overlapping but instead will share some members. Therefore, we investigate how neighborhood flow coupling handles overlap compared to full coupling. We begin by considering the simplest possible example: two identical, fully connected communities of size  $N$  that overlap by a fraction  $\delta$  (Fig. 2.a.) In this network, a random walker traversing the network occupies a node  $i$  inside the overlap with probability  $\delta$  and performs a relax step with probability  $r$ . Consequently, the random walker switches layer with probability

$$P^{\leftrightarrow} = \delta r \frac{D_i^{\alpha\beta}}{D_i^{\alpha\beta} + 1}. \quad (5)$$

A higher  $P^{\leftrightarrow}$  corresponds to stronger coupling between the two communities and increased preference for classifying the two as a single community. For full or adjacent coupling,  $D_i^{\alpha\beta} = 1$  and  $P_{FC}^{\leftrightarrow} = 1/2\delta r$ . Instead, for neighborhood flow coupling,  $D_i^{\alpha\beta}$  from (1) for a node in the overlap yields

$$P_{NFC}^{\leftrightarrow} = \delta r \frac{(\delta N - 1)}{(\delta N - 1) + (N - 1)}. \quad (6)$$

That is, the probability of switching layers is the fraction of time steps that a random walker can switch,  $\delta r$ , multiplied by the probability that a relax step will result in a layer switch (which is the number of nodes the walker can reach in the other layer divided by the total number of nodes the walker can reach when inside the overlap).

Figure 2.b shows  $P^{\leftrightarrow}$  as a function of  $\delta$  for full and neighborhood flow coupling at relax rate  $r = 1$ . This simple exercise reveals that the layer switching probability differs significantly in the important range  $\delta \in ]0, 0.5]$ , emphasizing that neighborhood flow coupling has a lower tendency to merge overlapping communities compared to both full coupling and adjacent layer coupling.

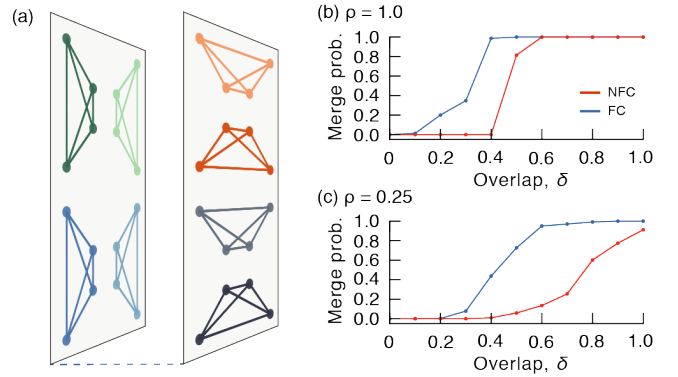


FIG. 3. **Full coupling merges communities at lower overlap.** (a) Schematic illustration of two layers of cliques with variable overlap. (b) The probability that Infomap with different coupling schemes merges two communities in separate layers as a function of their node overlap. (c) Same as (b) but for sparser networks, in which all but a fraction of  $\rho = 0.25$  links are randomly removed.

Let us now compare neighborhood flow coupling and full coupling in a more complex scenario. To investigate the threshold of overlap at which the two methods collapse overlapping communities, we construct a network benchmark model with 500 physical nodes partitioned into 50 communities of (uniform) size 10. The network has two layers and the partitions in each layer differ by some number of random edge swaps (Fig. 3.a). Using Infomap with both coupling schemes on 1000 network realizations, we record the overlap for each pair of communities in different layers and whether or not Infomap merges them (Fig. 3.b). We see that full coupling merges communities more aggressively than neighborhood flow coupling—in some cases, even when they only overlap by two nodes. Conversely, Infomap with neighborhood flow coupling requires substantial overlap before it merges two distinct communities.

In real-world networks, communities are sometimes sparsely linked internally. Since the neighborhood flow coupling considers overlap in internal link structure rather than in nodes, the likelihood of merging partly overlapping communities decreases with increasing sparsity. We observe this decline by repeating the simulation at density  $\rho = 0.25$ , with 75 percent of the edges randomly removed from each community (Fig. 3.c).

In real-world scenarios, there is no general right or wrong answer to the question of when two overlapping communities should be given a single label. As we have shown here, even when two communities overlap entirely, there is a small chance that they are not merged when the internal link structure is random and sparse. The network under study and the research question at hand should determine which coupling method is best. When the goal is to identify intermittent communities among many layers, it is important to avoid spurious community merges, and neighborhood flow coupling performs better at this task.

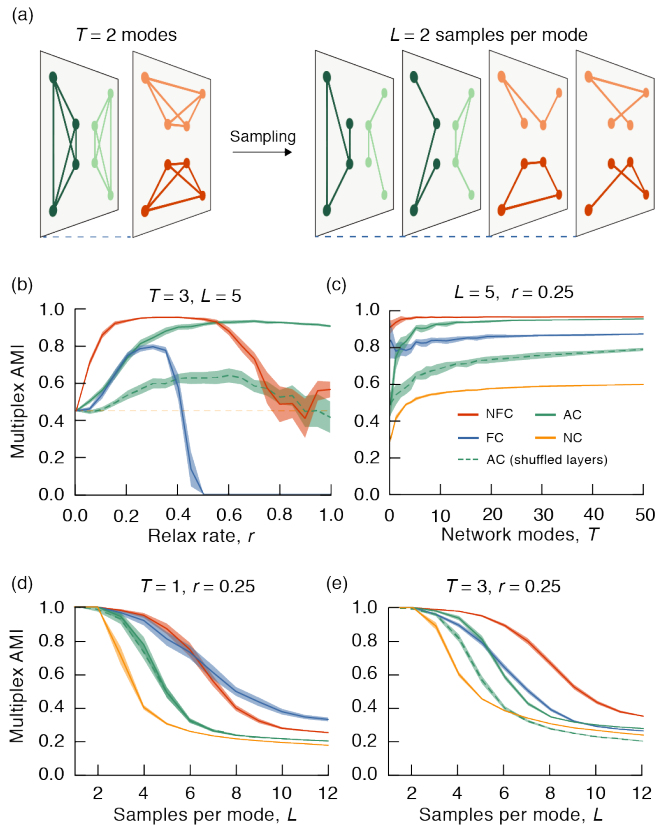


FIG. 4. **Neighborhood flow coupling captures intermittent overlapping communities in sparse multilayer LFR benchmark networks.** (a) Illustration of benchmark network for measuring performance in sparse networks with overlapping intermittent communities in  $T$  network modes and  $L$  sampled layers per mode. (b) Performance of all coupling methods measured by the AMI between the recovered and true partitions as a function of the relax rate  $r$ . We have dashed the line for no coupling to highlight that with constant  $r = 0$  by definition it does not depend on the relax rate. (c) Performance test for  $L = 5$  layers per mode and increasing number of network modes  $T$ . (d-e) Performance test for fixed number of network modes  $T = 1$  and  $T = 3$ , respectively, and increasing number of increasingly sparse sampled layers  $L$  per network mode. For more than one network mode, neighborhood flow coupling stands out as the best coupling method.

#### Intermittent communities

In networks with many layers, communities may persist over some period of time, then vanish and reemerge again by activating the same subset nodes with similar within-group link structures. Here we compare how different coupling schemes perform with respect to detecting such structure in increasingly sparse multi-mode benchmark networks [13]. First we generate  $T$  modes as independent LFR benchmark networks [24], with 128 nodes of average degree 16 divided into 4 equally sized communities. From each mode we independently sample  $L$  network layers that include links from their mode with probability  $1/L$ . Each multilayer benchmark network thus comprises  $T \times L$  layers, with  $T$  sets of  $L$  dependent

layers. Figure 4a illustrates a simplified rendering of this multilayer benchmark network with  $T = L = 2$ . With increasing  $L$  and sparser communities, the challenge is to detect the four communities planted in each mode and distinguish between communities from different modes.

To measure performance, we compute the adjusted mutual information [25], AMI, between the predicted and true state node labels. We first show that neighborhood flow coupling is less sensitive to variations in the relax rate (Fig. 4b). The no-coupling method is independent of the relax rate and serves as a performance baseline. For adjacent coupling, the performance increases with the relax rate because this coupling takes advantage of the ordered layers and completes information in sparse layers. However, when shuffling the layers, this advantage vanishes and the performance remains low for all relax rates. Full coupling has a narrow performance optimum and the performance drops to zero because the communities are washed out when all layers become strongly coupled. Neighborhood flow coupling is more stable and performs best with a relax rate between 0.15 and 0.4 for this type of multilayer network. We use  $r = 0.25$  as the default relax rate throughout our analysis.

For all types of coupling, performance depends on the number of network modes. On single-mode multilayer networks, neighborhood flow and full coupling perform similarly and better than no or adjacent coupling (Fig. 4d). We expect this result, as each state node only belongs to a single non-overlapping community. With an increasing number of samples per mode, the networks become sparser and the probability of finding high-similarity neighborhood flows decreases. As a result, neighborhood flow coupling converges to no coupling. However, multiple modes are not a problem for neighborhood flow coupling. In the three-mode multilayer networks with overlapping communities, the performance for full coupling drops to a level comparable to no and adjacent coupling, while neighborhood flow coupling maintains the same level of performance (Fig. 4e). In fact, the performance of neighborhood flow coupling remains stable for a much higher number of network modes (Fig. 4c). The dashed green line shows the performance of adjacent coupling with randomized layer order and therefore intermittent communities, illustrating that the high performance of adjacent coupling requires communities without interruptions. No other coupling method depends on the layer order. While all coupling methods maintain relatively high performance, neighborhood flow coupling stands out as the best method for intermittent communities.

#### Flow persistence

We have developed the neighborhood flow coupling to constrain flows within structurally similar overlapping regions of a network. To explore this feature using synthetic networks, we use a multilayer benchmark network model consisting of two signal layers with identical and known clusterings at both sides of a noise layer that, at a tunable degree, is independent of the signal layers (Fig. 5a). We generate the identical sig-

nal layers as LFR benchmark networks with 128 nodes in 8 equally sized communities with average degree 16 and per-node inter-community link probability 0.05, such that the expected number of links is  $n_e = 16(16 - 1)/2 \times 8 = 860$  [24]. The noise layer contains  $n_e(1 - \lambda)$  edges from the signal network and  $n_e\lambda$  edges from an independent network that we generate from the same model. By tuning  $\lambda$  from 0 to 1 we can gradually convert the noise layer from the signal network copy to an independent network [26]. We can now test how well different coupling methods handle interference from the noise layer by measuring the decrease in average adjusted mutual information between the identified signal and noise layer partitions as  $\lambda$  is increased.

Neighborhood flow coupling and no-coupling are robust to interference from irrelevant layers. When the noise layer is more than 80 percent independent of the signal layer, the partition overlap vanishes for both coupling methods. However, full and adjacent coupling suffer from interference with the noise layer even when it is independent of the signal layers (Fig. 5b). The strong coupling between signal and noise layers for these methods induces interlayer flows in spurious communities. Obviously, the no-coupling method is immune to such interference, and therefore is unable to pick up actual interlayer coupling in intermittent communities (Fig. 4). In contrast, neighborhood flow coupling is able to both avoid interference from irrelevant structures and pick up information from intermittent communities.

Neighborhood flow coupling can retain flows in intermittent communities. The proportion of flow inside the signal layers explains why neighborhood flow coupling outperforms full and adjacent coupling. In this three-layer example, for any uniform coupling scheme—be it full, adjacent or no coupling—each layer carries one third of the total flow, independent of  $\lambda$ . Therefore, two-thirds of the total flow in the signal layers forms a baseline. For neighborhood flow coupling, however, this fraction increases as  $\lambda$  approaches 1 and the signal and noise layers disentangle (Fig. 5c). The adaptive coupling reinforces flows inside the two signal layers together and prevents flows from leaking to the noise layer. As a result, neighborhood flow coupling accentuates structures with long flow persistence times across layers and makes it possible to detect intermittent communities in multilayer networks.

### Understanding real-world temporal contact networks

We now apply multiplex Infomap using neighborhood flow coupling, full coupling, adjacent coupling and no-coupling schemes to two empirical temporal contact networks. The first network represents contact events during working hours (approximately 8 a.m. to 6 p.m) between employees in a workplace environment over two weeks [20]. In this network there are  $n = 92$  physical nodes,  $e = 2.91 \cdot 10^3$  intralayer links,  $t = 575$  non-empty layers, and the average intralayer node degree is  $\langle k \rangle = 0.110$ . The second network arises from Bluetooth signal connections between personal smartphones of freshmen university students, also over two weeks [21] ( $n = 636$ ,  $e = 1.27 \cdot 10^5$ ,  $t = 600$ ,  $\langle k \rangle = 0.665$ ). In the uni-

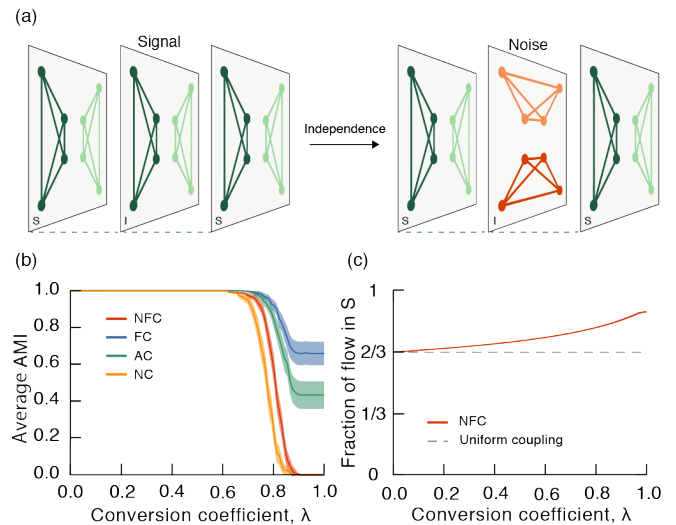


**FIG. 5. Neighborhood flow coupling amplifies flow persistence in communities.** (a) Schematic benchmark network for testing network flow persistence in planted communities. Two identical signal layers sandwich a noise layer with varying overlap, with the signal layers set by conversion coefficient  $\lambda$ , from identical at  $\lambda = 0$  to independent at  $\lambda = 1$ . (b) The average AMI between the identified partitions in the signal and noise layers decreases as they disentangle. (c) The fraction of total network flows captured by nodes in the signal layers increases as the signal and noise layers disentangle for neighborhood flow coupling, but is constant at two-thirds of the total flow for the uniform coupling methods. We use relax rate  $r = 1$  for neighborhood flow coupling to maximize interlayer flows and emphasize the effect.

versity dataset, links are tracked during a special study period where each student attends the same course every day. The students may meet anytime during the 24 hours of the day, but to simplify the comparison to the workplace network, we only consider links that occur during working hours (8 a.m.–4 p.m.). In each network, we aggregate links into layers that represent interactions in 10-minute intervals, and only layers between the first and last daily activity are used. We start by analyzing the interlayer link structure that neighborhood flow coupling produces. In particular, we are interested in understanding the sparsity of the representations that the method creates, compared to other methods. We then evaluate the performance of Infomap resulting from each coupling scheme by measuring overlap, size, and self-similarity over the time of communities that each method finds. There is no ground truth to measure performance against, so we focus our analysis on showing that neighborhood flow coupling strikes a balance between allowing information to flow between all layers—the strength of full coupling—and not mixing unrelated contexts—the strength of no coupling. Finally, we explore each network by visualizing the neighborhood flow coupling community detection solution.

*Neighborhood flow coupling finds communities that are highly self-similar*

We know from the literature that these networks contain intermittent communities [6, 27]. Therefore these networks are useful to better understand each different coupling method's ability to capture intermittent community structure. Due to the frequent daily re-emerging of communities, a method that couples temporally distant layers should cause the rate of new communities discovered on each day,  $p_{new}$ , to decline over time. This is indeed the case for full coupling and neighborhood flow coupling (Fig. 6.a-b). Full coupling drives  $p_{new}$  close to zero, which is unrealistic as we should expect some degree of exploration to take place. The reason for this behavior is likely the fact that new communities are merged with previous, slightly overlapping communities. For neighborhood flow coupling, intermittent communities are appropriately recognized each day, while a significant fraction of new configurations is given new labels.

Knowing that communities are indeed successfully rediscovered each day, we now seek to understand how self-similar intermittent communities are between days of (re)discovery. A good detection algorithm should partition the network such that each reappearance of a community is highly self-similar to its other appearances. We measure the similarity between each temporal community to itself on the most recent previous day as the cosine similarity between the unnormalized 24-hour aggregate distributions of member nodes, and plot the similarity distribution over time as their means inside the 95% confidence intervals. It is only relevant to measure self-similarity for full and neighborhood flow coupling, since only those two methods are able to capture reoccurring communities. In both networks, neighborhood flow coupling results in, on average, higher community self-similarity than full coupling does (Fig. 6.c-d). This difference is more pronounced in the university network because the structures are larger. In the case of full coupling, large communities are frequently split into smaller ones that are rarely detected.

*Full-coupling solutions tend to merge overlapping communities*

We measure the distribution of node entropy,  $P(S)$ , and the distribution of community size,  $P(\epsilon)$ , in each network. We compute the node entropy as  $S = \sum_i c \log c_i$  where  $c$  is the distribution over time spent in communities  $i$  for a given node. Intuitively, if the average node entropy is high, nodes are detected as frequently being in different communities, meaning that communities must overlap on many nodes. Full coupling results in low node entropy and large communities (see Fig. 6.c-e). In conjunction with our previous observation that full coupling leads to unrealistically low values of  $p_{new}$ , this is a strong indication that it causes Infomap to merge communities that overlap in different layers.

For both networks, the  $p_{new}$  curve for neighborhood flow coupling is similar to full coupling but with more new communities emerging each day. In the workplace network, we note that there are almost as many new communities discov-

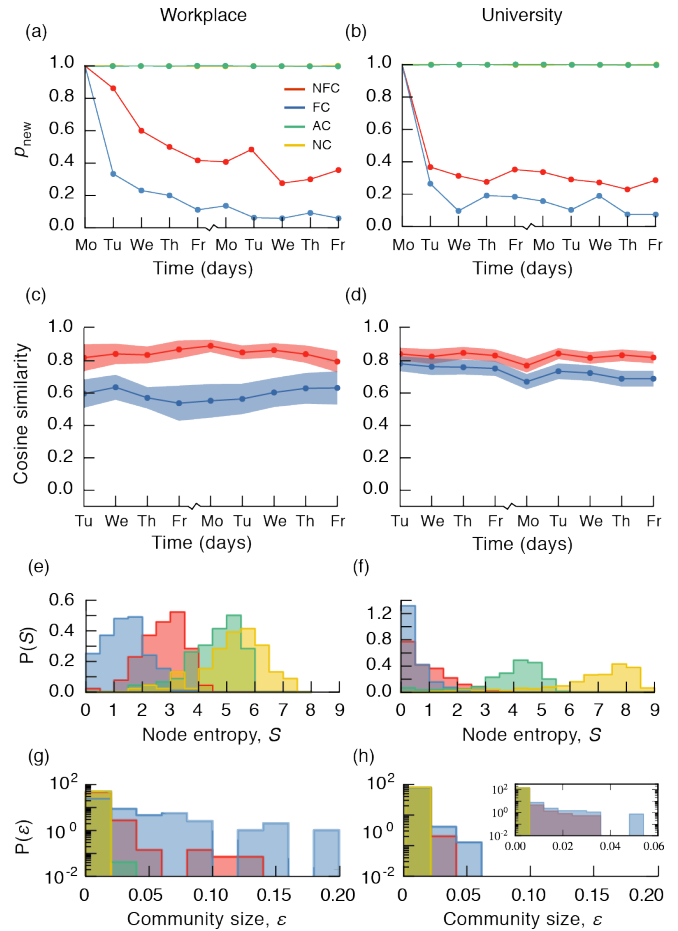


**FIG. 6. Properties of communities in real-world networks.** Each column corresponds to its own different network. (a-b) The number of new communities on each day,  $p_{new}$ , in the solutions for each coupling scheme. (c-d) Average community self-similarity over time. (e-f) Distribution of node community assignment entropy,  $S$ , as a measure of community overlap. (g-h) Community size distributions.

ered on the second day as there are on the first. We can explain this with the observation that the workplace dataset contains groups that are scheduled to meet every other day and, as such, we should expect some of those to start on the second day. While neighborhood flow coupling captures this nuance, full coupling does not. In the university network, neighborhood flow coupling identifies fewer and fewer communities as the week progresses, with the exception of Fridays, where relatively more new communities form. This nuance is not captured by full coupling. These results further support the concept that full coupling results in mergers of overlapping communities due to interlayer links that connect them via the nodes they overlap on.

*Visualization of temporal communities*

We visualize the temporal expansion and contraction of communities found by Infomap with neighborhood flow layer

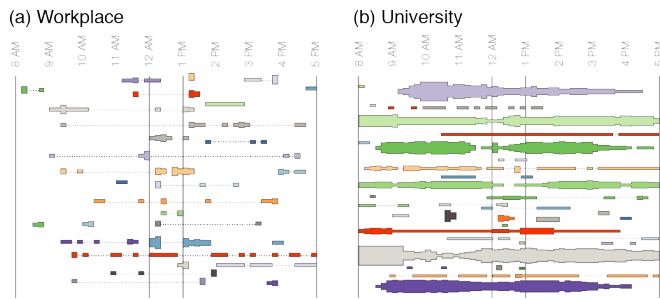


FIG. 7. **Temporal communities detected by Infomap with neighborhood flow coupling.** Each horizontal track represents a community and its varying height represents the number of active nodes over time. (a) Partition of the workplace network. Height to scale with (b). (b) Partition of the university network. At its tallest point, the largest community (top purple, 10 am) has 22 active members.

coupling in each network, as horizontal “strips” of varying height[28]. Fig. 7 displays a subset of the communities discovered in each network (vertical position is arbitrary). There are clear differences between the community structure of the two networks. The university network gives rise to large structures that persist over long periods of time, while the workplace communities are significantly more intermittent, lasting on the order of tens of minutes. Community sizes agree with our insight from Fig. 6.g-h. In the university network, some are large, corresponding to students attending lectures, some are mid-sized, corresponding to work-groups and small lectures, and some are small, corresponding to 2–4 person gatherings. In the workplace network, communities mostly consist of a few people and occasionally are larger around lunch, but never in a scale similar to the university, as we should expect. With these levels of intermittent communities—here observed in particular for the workplace network but also strongly present in the university network at a daily rate—it is clear that neighborhood flow coupling is a good choice for estimating layer interdependency. This visualization does not, however, inform us about overlap. Therefore we provide an interactive version of this visualization where the reader can hover over each community to display the other communities it overlaps with on a given day. The interactive version can be found at [http://ulfaslak.com/research/temporal\\_](http://ulfaslak.com/research/temporal_)

communities/.

## CONCLUSION

Our experiments suggest that connecting state nodes across layers in multilayer networks based on the similarity between their network neighborhood flows has multiple benefits over uniform entire-layer coupling approaches. For example, in series of timestamped face-to-face interaction events represented as multilayer networks, neighborhood flow coupling captures natural constraints on information flows such that flows move freely only within and between similar communities across layers. As a result, Infomap is able to identify intermittent communities with long flow persistence times and recognize spuriously overlapping communities as separate entities. In contrast, existing uniform entire-layer approaches either fail to capture whole communities that are intermittent across temporal layers or collapse spuriously overlapping communities into single communities. Furthermore, we demonstrate that neighborhood flow coupling results multilayer network representations that are order of magnitudes sparser in typical real-world networks with corresponding computational gains. This computational gain allows us to analyze and identify intermittent communities in temporal networks over longer times or higher resolution. Consequently, neighborhood flow coupling opens new avenues for temporal network analysis.

## ACKNOWLEDGMENTS

We thank Chris Blecker and Ludvig Bohlin for comments that improved our manuscript. M.R. was supported by the Swedish Research Council, grant 2016-00796. SL was funded by the Danish Council for Independent Research, grant number 4184-00556a, and the Villum Foundation ‘High resolution networks’. University contact data (from the Copenhagen Networks Study [21]) was collected with the permission of the Danish Data Protection Agency (Journal number 2012-41-0664).

- 
- [1] G. Palla, A.-L. Barabási, and T. Vicsek, *Nature* **446**, 664 (2007).
  - [2] C. Tantipathananandh, T. Berger-Wolf, and D. Kempe, in *Proceedings of the 13th ACM SIGKDD international conference on Knowledge discovery and data mining* (ACM, 2007) pp. 717–726.
  - [3] A.-K. Pietiläinen and C. Diot, in *Proceedings of the thirteenth ACM international symposium on Mobile Ad Hoc Networking and Computing* (ACM, 2012) pp. 165–174.
  - [4] J. Kauffman, A. Kittas, L. Bennett, and S. Tsoka, *PloS one* **9**, e101357 (2014).
  - [5] J. He and D. Chen, *Physica A: Statistical Mechanics and its Applications* **429**, 87 (2015).
  - [6] V. Sekara, A. Stopczynski, and S. Lehmann, *Proceedings of the national academy of sciences* **113**, 9977 (2016).
  - [7] L. Gauvin, A. Panisson, and C. Cattuto, *PloS one* **9**, e86028 (2014).
  - [8] L. Speidel, T. Takaguchi, and N. Masuda, arXiv preprint arXiv:1503.05641 (2015).
  - [9] T. P. Peixoto, *Physical Review E* **92**, 042807 (2015).
  - [10] C. Matias and V. Miele, *Journal of the Royal Statistical Society: Series B (Statistical Methodology)* (2016).
  - [11] P. J. Mucha, T. Richardson, K. Macon, M. A. Porter, and J.-P. Onnela, *science* **328**, 876 (2010).
  - [12] Y. Chen, V. Kawadia, and R. Urgaonkar, arXiv preprint arXiv:1303.7226 (2013).

- [13] M. De Domenico, A. Lancichinetti, A. Arenas, and M. Rosvall, *Physical Review X* **5**, 011027 (2015).
- [14] M. Bazzi, M. A. Porter, S. Williams, M. McDonald, D. J. Fenn, and S. D. Howison, *Multiscale Modeling & Simulation* **14**, 1 (2016).
- [15] D. B. Larremore, A. Clauset, and C. O. Buckee, *PLoS computational biology* **9**, e1003268 (2013).
- [16] N. Stanley, S. Shai, D. Taylor, and P. J. Mucha, *IEEE Transactions on Network Science and Engineering* **3**, 95 (2016).
- [17] C. De Bacco, E. A. Power, D. B. Larremore, and C. Moore, *arXiv preprint arXiv:1701.01369* (2017).
- [18] M. Rosvall and C. T. Bergstrom, *Proceedings of the National Academy of Sciences* **105**, 1118 (2008).
- [19] M. Rosvall, D. Axelsson, and C. T. Bergstrom, *The European Physical Journal Special Topics* **178**, 13 (2009).
- [20] M. Génois, C. L. Vestergaard, J. Fournet, A. Panisson, I. Bonmarin, and A. Barrat, *Network Science* **3**, 326 (2015).
- [21] A. Stopczynski, V. Sekara, P. Sapiezynski, A. Cuttone, M. M. Madsen, J. E. Larsen, and S. Lehmann, *PLoS one* **9**, e95978 (2014).
- [22] J.-C. Delvenne, S. N. Yaliraki, and M. Barahona, *Proceedings of the National Academy of Sciences* **107**, 12755 (2010).
- [23] U. Braun, A. Schäfer, H. Walter, S. Erk, N. Romanczuk-Seiferth, L. Haddad, J. I. Schweiger, O. Grimm, A. Heinz, H. Tost, *et al.*, *Proceedings of the National Academy of Sciences* **112**, 11678 (2015).
- [24] A. Lancichinetti, S. Fortunato, and F. Radicchi, *Physical review E* **78**, 046110 (2008).
- [25] N. X. Vinh, J. Epps, and J. Bailey, *Journal of Machine Learning Research* **11**, 2837 (2010).
- [26] R. Aldecoa and I. Marín, *arXiv preprint arXiv:1306.4149* (2013).
- [27] J. Stehlé, N. Voirin, A. Barrat, C. Cattuto, L. Isella, J.-F. Pinton, M. Quagiotto, W. Van den Broeck, C. Régis, B. Lina, *et al.*, *PLoS one* **6**, e23176 (2011).
- [28] U. A. Jensen, “How people gather: An interactive visualization approach,” <http://www.sciencemag.org/projects/data-stories/winners> (2016).

### Appendix A: Interlayer sparsity

To couple state nodes, neighborhood flow coupling requires that the network structure around state nodes be similar. This similarity is not required by full coupling, which couples state nodes of each physical node regardless. In temporal networks, there are often many state node pairs that have no structural similarity, because they can participate in non-overlapping communities at different times. With neighborhood flow coupling, this results in network representations with with sparse interlayer link structure compared to full coupling, where the interlayer network is always dense. In this appendix, we investigate the degree to which neighborhood flow coupling reduces the size of the network, and thus the memory footprint. We measure the density reduction in relation to the full-coupling density, which is always one, and compare to the adjacent coupling density. Furthermore, we analyze how density varies with layer interdependence for neighborhood flow coupling, as we reason that this must be an important factor.

First, we consider sparsity in synthetic networks with independent layers. We define interlayer density,  $S$ , as the ratio

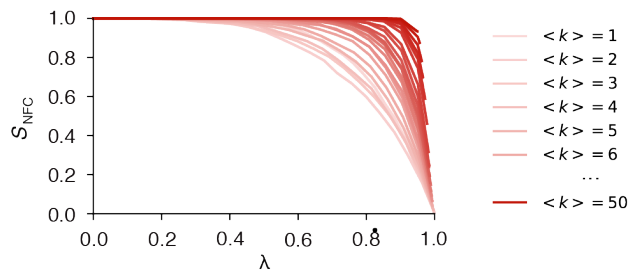


FIG. 8. **Interlayer sparsity depends on layer interdependence.** The density of interlayer links  $S_{NFC}$  created by neighborhood flow coupling decreases as the layers in a multilayer network become more independent (increasing  $\lambda$ ). The rate at which density decreases depends on the average degree of state nodes  $\langle k \rangle$ . Sparse intralayer link structure, corresponding to low  $\langle k \rangle$ , leads to sparser interlayer link structure.

of realized to possible interlayer links. Per definition, it is always the case that  $S_{FC} = 1$  and  $S_{NC} = 0$ . If layers are independent, we can derive  $S_{AC} = 2/t$  by dividing the expected number of links from adjacent coupling with the expected number of links from full coupling. For  $t = 600$  (corresponding to two weeks of working hours in 10-minute time-bins),  $S_{AC} = 3.3 \cdot 10^{-3}$ .  $S_{NFC}$  can be approximated as the probability that two state nodes have at least one link in common:

$$S_{NFC}(\langle k \rangle, n) = 1 - P\left(0, \frac{\langle k \rangle^2}{n}\right) = 1 - e^{-\langle k \rangle^2/n}, \quad (\text{A1})$$

where  $P(0, \theta)$  is the function value in 0 of a Poisson distribution with average  $\theta$  equal to the expected number of shared links between two state nodes in independent layers  $\langle k \rangle^2/n$ . For a network with similar statistics to the university network ( $n = 636$ ,  $\langle k \rangle = 0.665$ ), Eq. (A1) gives  $S_{NFC} = 7.0 \cdot 10^{-4}$ . In real temporal networks, however, we observe that the interlayer link structure is more dense because there is significant dependence between layers. The estimations presented here therefore only serve as random network baselines that we can compare with. For the university network, where the possible number of interlayer links is  $7.11 \cdot 10^7$ , we observe  $S_{NFC} = 0.680$  and  $S_{AC} = 0.005$ , and for the workplace network, where the possible number of interlayer links is  $4.33 \cdot 10^5$ ,  $S_{NFC} = 0.299$  and  $S_{AC} = 0.012$ . The large increase in  $S$  that we observe for the empirical networks reveals that neighborhood flow coupling is very sensitive to interdependence between layers.

We now test how sensitive interlayer sparsity resulting from neighborhood flow coupling is to layer interdependence, using a simple experiment similar to the approach taken in the *Flow persistence* section above. We create an Erdős-Rényi graph with  $n = 1000$  and variable  $\langle k \rangle$ . We create a two-layer network where both layers are copies of this network, such that the layer independence  $\lambda$ , which we measure as the average Jensen-Shannon divergence across all pairs of state nodes, is zero. We then gradually convert the second layer to an independent network, generated by the same process, using edge swaps, while measuring  $S_{NFC}$  versus  $\lambda$ . When the second

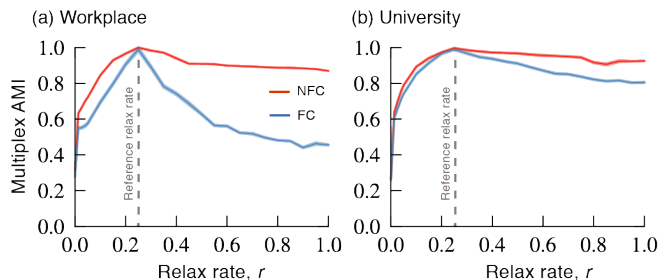


FIG. 9. **Neighborhood flow coupling is highly robust to variations in  $r$ .** The plots illustrate the similarity of a community detection solution using  $r = 0.25$  with solutions obtained from different relax rates. The high values for neighborhood flow coupling in both networks (a) and (b) demonstrate its high robustness to  $r$  variability compared to full coupling.

layer is fully converted, the two layers are maximally independent and  $\lambda = 1$ . The experiment shows, first of all, that the relationship between  $S_{NFC}$  and  $\lambda$  is non-linear. Secondly, we observe that a sparse intralayer structure (low  $\langle k \rangle$ ) leads to a sparser interlayer link structure, increasingly so when layers are independent (Fig. 8).

Thus neighborhood flow coupling offers significant gains in memory efficiency relative to full coupling, particularly in sparse multilayer networks.

#### Appendix B: Robustness to relax rate

The problem at hand should decide what relax rate  $r$  to use. In general, for full coupling,  $r$  must be large enough to facilitate flow between layers yet small enough to contain in-

formation inside the layer communities. For neighborhood flow coupling, this heuristic does not apply, because interlayer links are established only between structurally similar regions of the network. At the same time,  $r$  still controls the amount of interlayer flow in the network. If  $r = 0$ , information cannot flow between layers, and if  $r = 1$ , important layer information may be diluted.

The optimal relax rate  $r$  should allow Infomap to discover communities that repeat in different layers. To test this criterion, we perform a simple experiment that starts with a multilayer network, selects a random layer and appends a copy of it to the end of the network. For a range of  $r$  values, we then measure the proportion of nodes in the copied layer to which Infomap assigns the same label as in the original layer. We perform this test on the university and the workplace networks for neighborhood flow and full coupling, and find that both coupling schemes give perfect labeling of all copied nodes for all values of  $r$  except  $r = 0$ . While this result does not reveal a performance optimum for  $r$ , it shows that the map equation can effectively capture layer interdependences.

The results should not be sensitive to the exact choice of the relax rate. We demonstrate the robustness by clustering a network for a range of relax rates and comparing each solution to the solution for  $r = 0.25$ , with the multiplex AMI as a performance measure. If robustness is high, all solutions should have a high AMI with this reference solution. Performing this test for both networks, we find that neighborhood flow coupling solutions are significantly more robust to varying  $r$  than full-coupling solutions. Neighborhood flow coupling is particularly robust in the domain  $r > 0.25$ . The similarity decays faster when  $r < 0.25$  and goes to zero for  $r = 0$ , which demonstrates that, while robust to  $r$ , Infomap with neighborhood flow coupling allows for detecting smaller communities. In summary, a broad spectrum of relax rates gives similar solutions for Infomap with neighborhood flow coupling.